Optimal Water Allocation from Subsurface Dams: A Risk-Based Optimization Approach

Azizallah Izady[1*], *Mohammad Sadegh Khorshidi*[1], *Mohammad Reza Nikoo*[2], *Ali Al-Maktoumi*[1,3], *Mingjie Chen*[1], *Hilal Al-Mamari*[1], *Amir H. Gandomi*[4]

[1]*Water Research Center, Sultan Qaboos University, Muscat, Oman*

[2]*Dept. of Civil and Architectural Engineering, Sultan Qaboos University, Muscat, Oman*

[3]*Dept. of Soils, Water and Agricultural Engineering, College of Agricultural and Marine Sciences, Sultan Qaboos University, Muscat, Oman*

[4]*Faculty of Engineering and IT, University of Technology Sydney, Ultimo, NSW 2007, Australia*

[*]*Corresponding author email: az.izady@squ.edu.om*

ABSTRACT

Subsurface dams, strongly advocated in the 1992 United Nations Agenda-21, have been widely studied to increase groundwater storage capacity. However, an optimal allocation of augmented water with the construction of the subsurface dams to compensate for the water shortage during dry periods has not so far been investigated. This study, therefore, presents a risk-based simulation-optimization framework to determine optimal water allocation with subsurface dams, which minimizes the risk of water shortage in different climatic conditions. The developed framework was evaluated in Al-Aswad *falaj*, an ancient water supply system in which a gently sloping underground channel was dug to convey water from an aquifer via the gravity force to the surface for irrigation of downstream agricultural zones. The groundwater dynamics were modeled using MODFLOW UnStructured-Grid. The data of boreholes were used to generate a three-dimensional stratigraphic model, which was used to define materials and elevations of five-layer grid cells. The validated groundwater model was employed to assess the effects of the subsurface dam on the discharge of the *falaj*. A Conditional Value-at-Risk optimization model was also developed to minimize the risk of water shortage for the augmented discharge on downstream agricultural zones. Results show that discharge of the *falaj* is significantly augmented with a long-term average increase of 46.51%. Moreover, it was found that the developed framework decreases the water shortage percentage in 5% of the worst cases from 87%, 75%, and 32% to 53%, 32%, and 0% under the current and augmented discharge in dry, normal, and wet periods, respectively.

KEYWORDS: Subsurface dam; Water allocation; Conditional Value-at-Risk; Optimization; MODFLOW; *falaj*.

1. INTRODUCTION

Water is a scarce resource in most arid and semi-arid areas and, evidently, will become more limited in the future. Aggravated by the rapid increase in population, industrial growth, and effects of climate change, this issue will continue to exert significant pressure on the water resources. Therefore, efficient and well-planned water resource management is of crucial importance for sustainable development in arid and semi-arid environments (Nazarieh et al. 2018). Subsurface dams (also known as groundwater dams, underground dams, underground reservoirs, and groundwater storage dams) are strongly advocated in the 1992 United Nations Agenda 21 and have received great attention as alternative water supply systems with minimal environmental impacts (dos Santos Gomes et al. 2018).

Subsurface dams have been studied in the literature from different aspects, such as augmenting the availability of groundwater resources (e.g. Hut et al. 2008, Zarkesh et al. 2012; Du Preez 2018), controlling seawater intrusion (e.g. Nawa and Miyazaki 2009; Knorr et al. 2016; Armanuos et al. 2019), determining the optimum site for subsurface dams (e.g. Forzieri et al. 2008; Jamali et al., 2014; Rohina et al. 2020), modeling the changes of groundwater flow with the construction of the subsurface dams (e.g. Senthilkumar and Elango 2011; Lalehzari and Tabatabaei 2015; Kim et al. 2017), designing subsurface dams (e.g. Nishigaki et al. 2004; Kabiri-Samani and Shams 2014), treating groundwater contamination (e.g. Bondoc 1986; Al-Nahari 2004), assessing the impact of subsurface dams on groundwater quality (e.g. Ishida 2006; Li et al. 2019), and investigating the effect of climatic changes on subsurface dams (e.g. Adham 2011).

Although the impact of subsurface dams on groundwater flow has been investigated in several studies, they failed to investigate properly the optimal allocation of augmented water with the construction of the subsurface dam to the downstream agricultural demands. In fact, how much the construction of the subsurface dam has compensated for the water shortage during the dry periods has not so far been

investigated. Therefore, this study, as a first attempt, presents a risk-based optimization framework to determine the optimal agricultural water allocation with the construction of the subsurface dam, which minimizes the risk of water shortage in different climatic conditions.

The developed framework was evaluated in the Al-Aswad *falaj* in Muscat, Oman. A *falaj* (plural *aflaj*) (also known as *qanat* (Iran), *qanat romani* (Jordan and Syria), *karez* (Afghanistan and Pakistan), *kanerjing* (China), *khettara* (Morocco), *foggara* (North Africa), *galerias* (Spain)) is an ancient water supply system in which a gently sloping underground channel is dug in the earth to convey water from an aquifer through the gravity force to the surface (more details are provided in the Supplementary Information (SI), section 1). A key concern of the *aflaj* is the loss of excess flow during the high rainy seasons, in which there is little need for the downstream agricultural demands. As a major focus, this study addresses how this surplus water can be stored with the construction of the subsurface dam and then used during the dry periods. Therefore, the following gaps, which have not been addressed in prior investigations, are the objectives of this study:

- To conduct a groundwater flow simulation using MODFLOW-UnStructured Grid.
- To assess the effects of the subsurface dam on the groundwater flow.
- To develop a risk-based optimization model to minimize the risk of water shortage under different climatic conditions.

2. DATASET AND METHODOLOGY

This study was undertaken in three steps: i) develop a groundwater model using MODFLOW-UnStructured Grid; ii) assess the effects of the subsurface dam on the discharge of the Al-Aswad *falaj* using calibrated and validated groundwater model; and iii) develop a risk-based optimization model to

determine an optimal irrigation scheduling for the augmented discharge of the *falaj* using the concept of Conditional Value-at-Risk (CVaR) for different climatic conditions.

2.1. GROUNDWATER MODELING

2.1.1. STUDY AREA AND GROUNDWATER MODELING DOMAIN

Al-Aswad *falaj*, served as the study area, is located at the wadi (catchment) Mayh, northeast of Oman (Fig. 1a and b). Since determining an appropriate set of boundary conditions was difficult to develop a groundwater model specifically for the Al-Aswad *falaj*, a large-scale groundwater model was first developed using MODFLOW-USG (Panday et al. 2013). Then, the cells were refined near the *falaj* for more realistic modeling of the effects of the subsurface dam on the *falaj's* discharge. The groundwater modeling domain is approximately 1,264 km^2 and between 58°18′ E and 58°42′ E longitude and 23°11′ N and 23°31′ N latitude. Rainfall is highly localized, in which annual mean rainfall ranges from less than 100 mm along the coast to over 200 mm in the mountains. This low and erratic rainfall, accompanied by a high potential evaporation of about 2,150 mm yr^{-1} results in arid to semi-arid conditions (Gibb 1976).

2.1.2. GEOLOGY AND HYDROGEOLOGY

Groundwater modeling domain is geologically dominated by the southern portion of the Northern Oman Mountains (NOMs), which meet the Oman Sea along a typically rugged coastline. The oldest rocks, Huqf Group (pre-Permian), dominate the southern and southeast parts of the study area lying within the catchments of wadis Aday and Mayh. The Hajar Super Group (HSG) (Permian to Cretaceous) is typically carbonate-dominated with massively bedded rocks that form the highest topography in the study area. The Ophiolite Nappes are limited to the northern edge of the study area. Tertiary limestone

outcrops in the northeast and northwest of the study area, which are mainly comprised of micritic, nodular and bioclastic limestones, subordinate conglomerates, sandstones, and marls. Quaternary lithologies are scattered throughout the study area and along the coast. These deposits are typically represented by very ancient to sub-recent alluvial fans and terraces, sub-recent to recent piedmont deposits, and ancient to recent slope colluvium. Recent wadi alluvium is present within active wadi channels crossing the region (Fig. 1b) (Glennie et al. 1974).

Groundwater primarily takes place in the Quaternary alluvial deposits that are restricted to the active wadi channels and also within the fractured/karstified bedrock of the HSG and Tertiary limestone. The Huqf Group is relatively impermeable and does not constitute productive aquifers. The rock types of the HSG have good secondary permeability associated with karstified and fissure/fault zones. Substantial fracturing and weathering in Ophiolite Nappe, which is especially well-developed in the coarse-grained peridotites, both at the surface and along the major fault and thrust zones, produce significant secondary porosity and permeability. The Tertiary limestone is heavily karstified in the study area so that it forms an important aquifer, and the alluvium composes the main aquifer in association with the weathered zone of the underlying bedrock. The alluvial aquifer provides the most demands of the study area, including the agricultural and urban development along the coast (Smith 1984; Macdonald 1985).

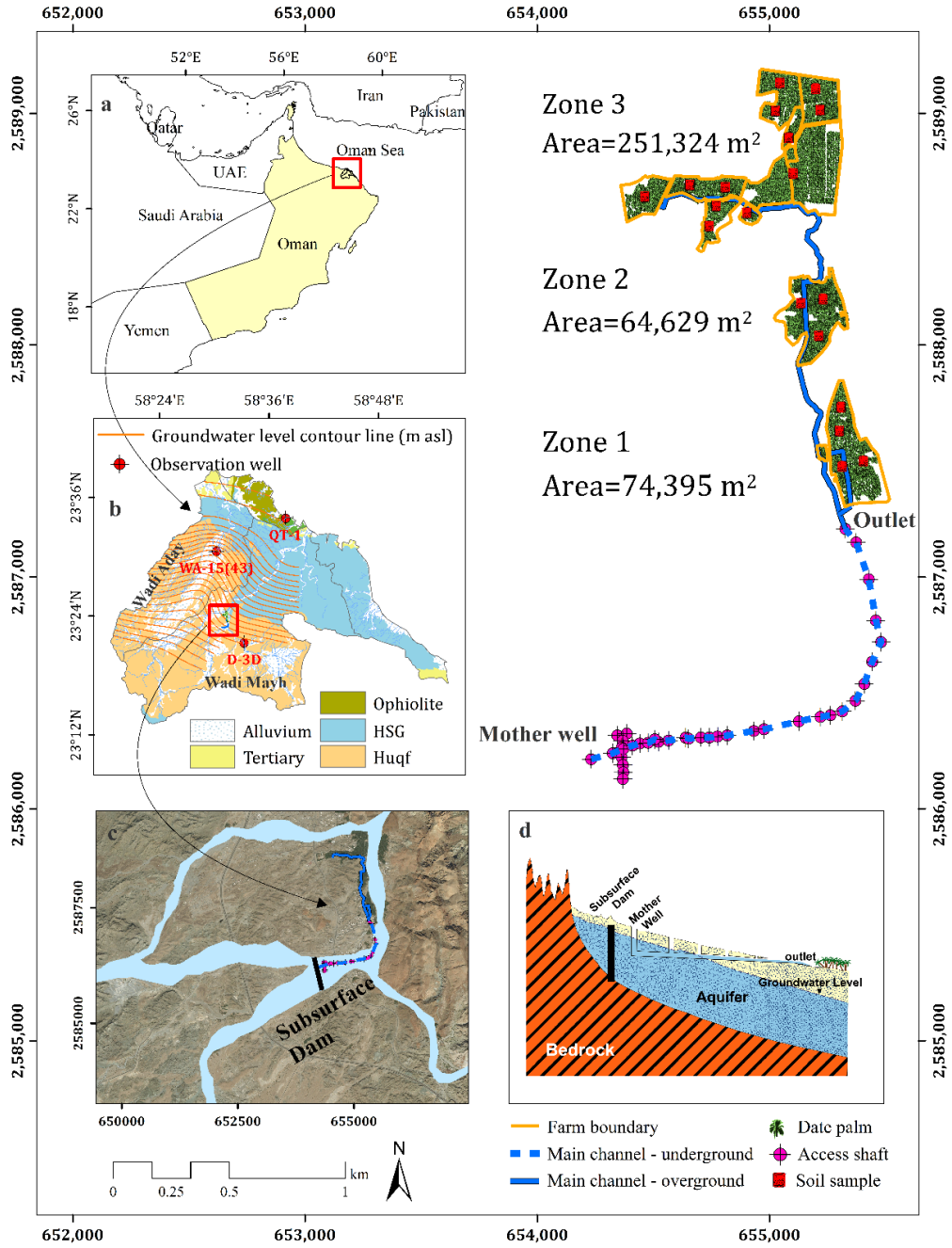

Fig. 1. *Al-Aswad falaj and three downstream agricultural zones. Sub-figures a and b shows the location of the Al-Aswad falaj in the northeast of Oman and in the Mayh catchment along with five principal geological units, wadis (ephemeral rivers) network, and groundwater level contour line. Sub-figure c displays the location of the subsurface dam, which is installed at the upstream of the mother well and across the wadi bed. Sub-figure d exhibits the schematic of the Al-Aswad falaj longitudinal cross-section in which the location of the subsurface dam, mother well, shafts and outlet are vividly shown.*

2.1.3. GROUNDWATER CONCEPTUAL MODEL

The framework proposed by Izady et al. (2014) was used for developing the groundwater conceptual model of the study area. The groundwater flow originates from the southwest of the study area and reaches to the northeast of the study area at sea level (Fig. 1b). The data of 90 boreholes were used to generate a three-dimensional stratigraphic model of the five principal hydrogeological units, including Huqf, HSG, Ophiolite, Tertiary, and alluvium geologic units (Fig. S2 in SI section 2). The thickness of the stratigraphic model ranges from 240 to 600 m throughout the study area, where the alluvium thickness varies between 20 and 74 m (Smith 1984; Macdonald 1985). According to the aquifer test results, the alluvium hydraulic conductivity varies between 20 to 100 m day^{-1} and specific yield ranges 0.05-0.15. The Tertiary geologic unit has a specific yield of 0.005 and hydraulic conductivity of 2.74 m day^{-1}, while those of the Ophiolite formation are 0.001 and 0.43 m day^{-1}. The HSG has the highest hydrodynamic properties compared with other hardrock formations, with a specific yield of 0.008 and hydraulic conductivity of 4.74 m day^{-1}. For the Huqf group, specific yield and hydraulic conductivity are estimated to be 0.15 m day^{-1} and 0.001, respectively. All required data for the groundwater modeling is obtained from the Ministry of Agriculture, Fisheries, and Water Resources, Oman.

2.1.4. GROUNDWATER MODEL STRUCTURE AND SETUP

MODFLOW-USG was employed to model groundwater flow which uses the control volume finite difference (CVFD) formulation (Panday et al. 2013). The model was first calibrated for the steady-state condition based on Jan. 1991 hydrologic conditions to determine the spatial distribution of groundwater levels and hydraulic conductivity. The calibrated groundwater levels and hydraulic conductivity were then used as initial conditions in the transient model, which was simulated for 26 years from Feb. 1991 to Dec. 2016. For the transient modeling, the time unit, time step, and stress period were specified as

daily, monthly, and monthly, respectively. The transient model was calibrated and validated from Feb. 1991 to Dec. 2014, and Jan. 2015 to Dec. 2016, respectively.

Materials and elevations of five-layer unstructured grid cells were obtained from a stratigraphic model. A smoothed Octree grid was used to refine the grid cells around the Al-Aswad *falaj* (Fig. 2). Model grid cells respectively range from 1000×1000 m and 500×500 m in hardrock and alluvium areas to 100×100 m in wadis and 50 m in the Al-Aswad *falaj*, where finer cells are required. The thickness of the cells varies from 240 to 600 m throughout the study area, in which the alluvial thickness ranges 20-74 m in the layers one to three. A constant head of zero is considered for the coastline boundary along the coast of the Oman Sea in the northeast of the study area. The highlands of the NOMs, which are situated at the southwest boundary of the study area, represent a groundwater and surface water divide. No-flux boundary condition is presumed for the east and west boundaries since they are parallel to the direction of the groundwater flow. The water-table fluctuation-based approach, proposed by Izady et al. (2017), was employed to estimate the recharge rates resulting from rainfall, runoff, evapotranspiration, abstraction, and leakage from the public water distribution network (Ahmadi et al. 2012, 2015). The estimated values were used as initial values for groundwater recharge in the modeling. The annual groundwater abstraction for irrigation and domestic consumptions is estimated to be 14.6 Mm^3 from the wells and 5.1 Mm^3 from the wellfield and was assigned in the model. The hydrodynamic values were entered the model for different geologic units. The Empirical Bayesian Kriging interpolation method was used to generate groundwater contour lines from the observation wells.

Calibration of the model was performed by changing the values of hydrodynamic parameters so that the simulated discharge of the Al-Aswad *falaj* and groundwater levels match the observed values. The response of the model to parameter changes was initially accomplished by trial and error. Then, the PEST algorithm (Doherty 1998) was used to achieve optimum values using the Al-Aswad *falaj* discharge and

observation wells. The Root Mean Square Error (RMSE) and coefficient of determination (R^2) were determined to assess the efficiency of the model.

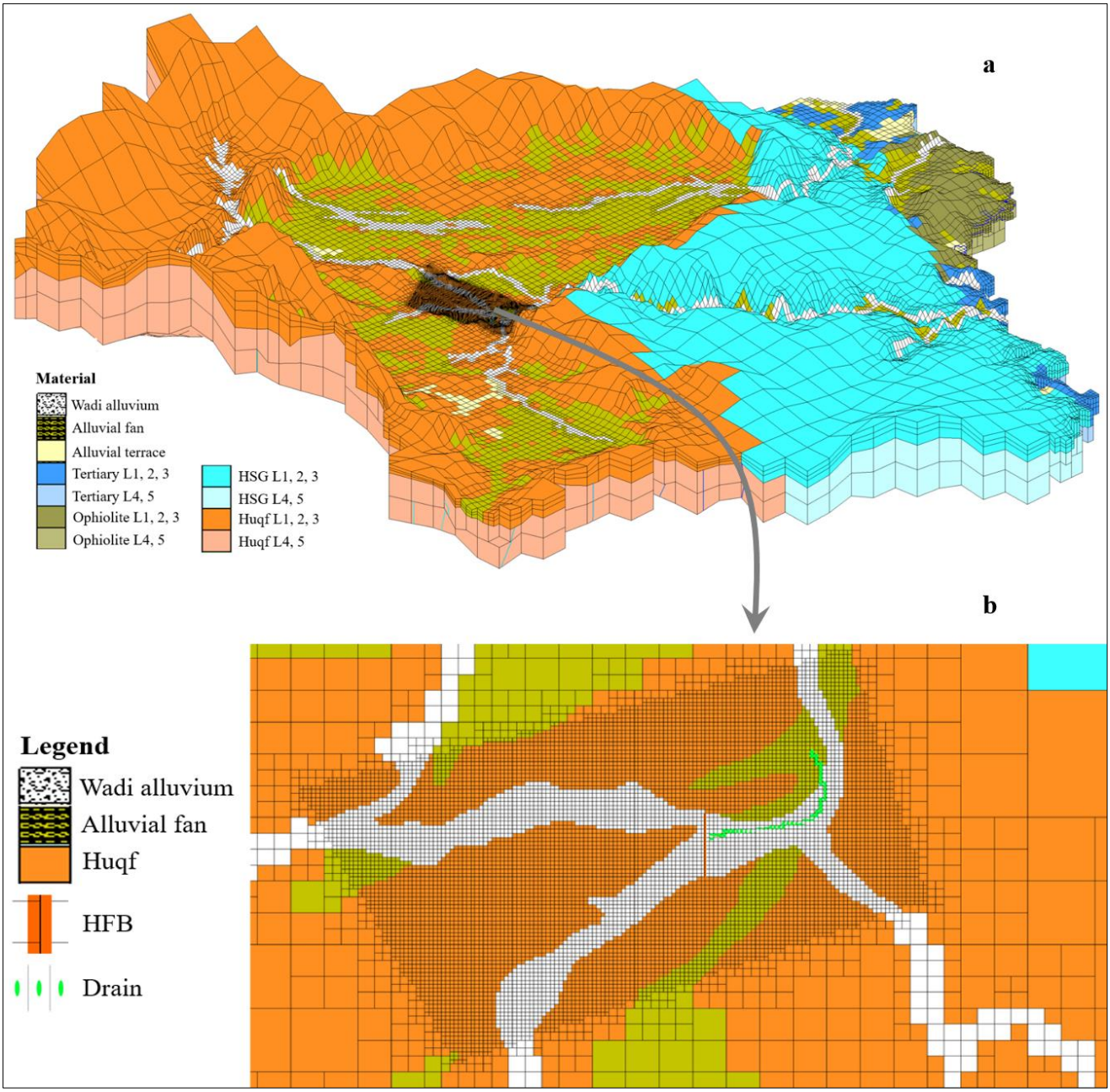

Fig. 2. *(a) Three-dimensional MODFLOW unstructured grid of the groundwater modeling domain along with the five layers and materials; (b) The locally refined grid around the Al-Aswad falaj and installed subsurface dam at the upstream of the mother well and across the wadi bed.*

2.2. SUBSURFACE DAM CHARACTERISTICS

The discharge of the Al-Aswad *falaj* was simulated using a drain package. Then, a horizontal flow barrier (HFB) package was employed to simulate the effects of a subsurface dam on the Al-Aswad *falaj* discharge. The subsurface dam is installed at upstream of the mother well and across the wadi bed. The alluvium is divided into three layers in the model (Fig 2), in which the subsurface dam is installed in the second and third layers. The subsurface dam facilitates raising the groundwater level so that the groundwater flows over the subsurface dam through layer 1 (Fig. 1d and Fig. 2b). The hydraulic conductivity and the subsurface dam thickness were estimated through trial-and-error to attain the maximum increase in discharge of the Al-Aswad *falaj*.

2.3. DEVELOPMENT OF THE RISK-BASED OPTIMIZATION MODEL

2.3.1. AL-ASWAD *FALAJ* DOWNSTREAM IRRIGATION WATER DEMAND

As shown in Fig. 1, the Al-Aswad *falaj* is the only water source for irrigation of three agricultural zones with a total area of 390,348 m^2. The crops cultivated in the area are date palm trees, corn silage, lemon, and banana, and the cultivation area of zones 1, 2, and 3 are 74,395, 64,629, and 251,324 m^2, respectively. 100%, 90%, and 85% of zones 1, 2, and 3 are respectively cultivated with an intercropping system of date palm and corn silage. The numbers of date palm trees in zones 1, 2, and 3 are 1,096, 1,117, and 3,410, respectively. There are 25 lemon trees in zone 3, of which 5% of the area is also cultivated with banana trees. A traditional basin surface irrigation method is practiced in the area, where its conveyance and application efficiencies are measured at 80% and 60%, respectively. The data and information were collected through several land surveys, field trips, laboratory tests, discussions with local farmers and experts and from the Ministry of Agriculture, Fisheries and Water Resources, Oman as well. Herein, we calculated the crops' water requirements based on the reference evapotranspiration

(ET_0) using the FAO Penman-Monteith equation (Allen et al. 1998). The calculations for the water requirements of different crops and zones are provided in the SI, section 3.

Traditionally, farmers' irrigation scheduling was determined based on the size of farmlands (controlled by the water share) and their participation in the construction and maintenance of *falaj* systems (Al Marshudi 2007). In fact, the currently applied irrigation scheduling, which has been used for a long time, is not based on the required irrigation water demand, leading to the significant overuse of irrigation water. According to this type of irrigation scheduling, regardless of the required irrigation demand and, more importantly, the climatic conditions (e.g. dry, normal, and wet), the farmers are allowed to have a full discharge of the *falaj* for irrigation of their farmlands during a specified time, known as the irrigation duration. Once all farmlands receive their share of water, it is repeated cyclically, which is known as the irrigation interval (or water cycle of the *falaj*). The irrigation duration and interval are collectively known as irrigation scheduling (IS). It is clear that the currently applied IS is not optimal, and therefore, a significant amount of irrigation water is overused. The currently used irrigation interval of the Al-Aswad *falaj* is six days, and the irrigation durations for zones 1, 2, and 3 are 1, 1, and 4 days, respectively. Fig. 3a shows the historical discharge of the Al-Aswad *falaj* from 1992 to 2015 and the calculated gross water demand of the three agricultural zones.

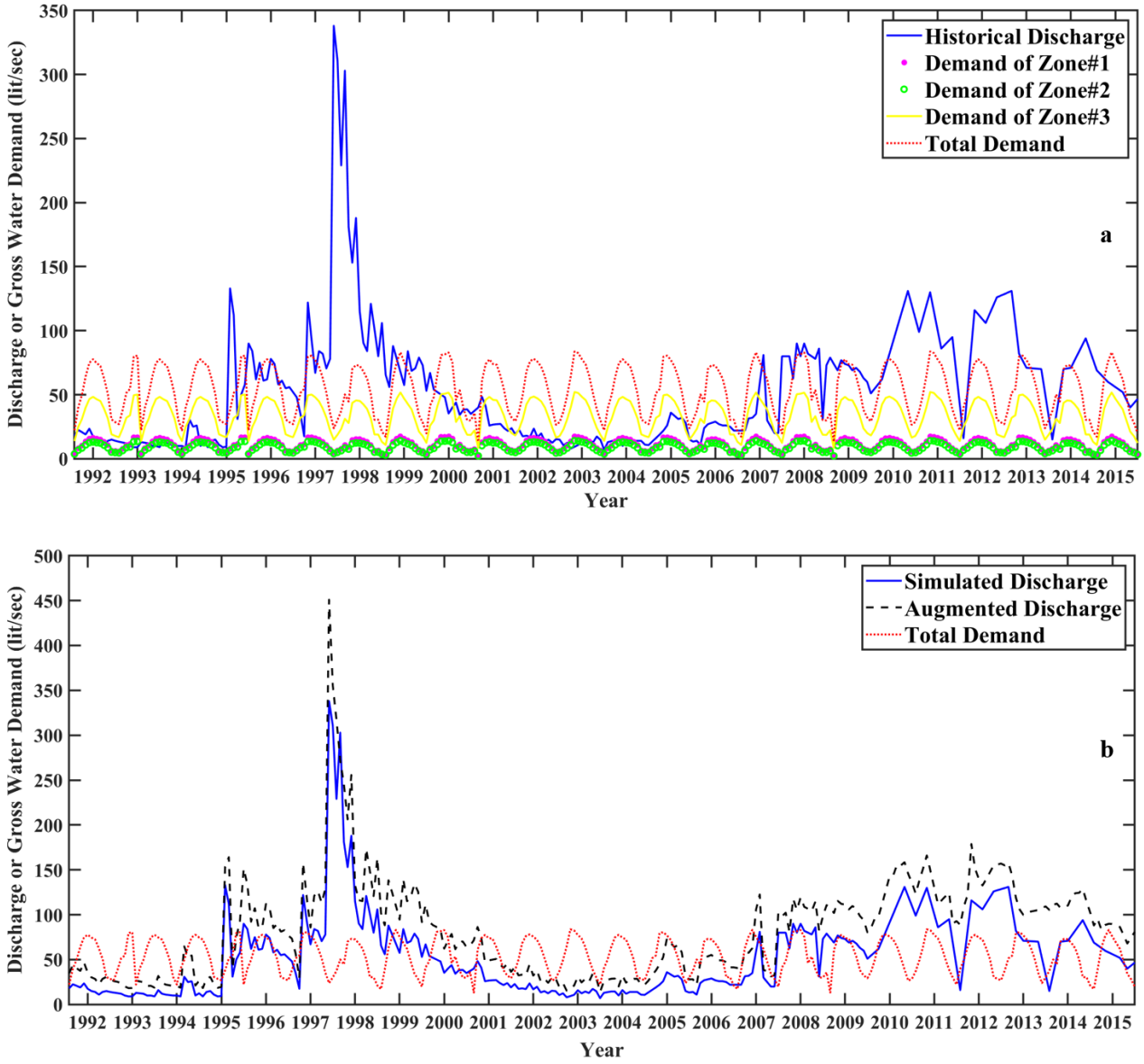

Fig. 3. *(a) The historical monthly discharge of Al-Aswad falaj and the individual and total monthly gross water demands of the three agricultural zones; (b) Plots of simulated discharge of Al-Aswad falaj before and after construction of the subsurface dam along with the total agricultural demand.*

2.3.2. RISK-BASED IRRIGATION SCHEDULING OPTIMIZATION MODEL

As mentioned earlier, the current IS of the agricultural zones downstream of the Al-Aswad *falaj* along with the *falaj*'s discharge has caused a significant amount of water shortage, especially during dry years.

The concept of Conditional Value-at-Risk (CVaR) was introduced by Rockafellar and Uryasev (2000) as a replacement for Value-at-Risk (VaR) to quantify and minimize the amount of risk associated with a decision considering the possibility of different outcomes (Izady et al. 2020). Therefore, the IS can be interpreted as a decision associated with various possible amounts of water shortage in the agricultural zones. Thus, the concept of CVaR is used to assess the impact of the augmented discharge of the Al-Aswad *falaj* with a subsurface dam on the downstream agricultural zones. Hereafter, we use the term "historical discharge" and "augmented discharge" for the real historical discharge of the Al-Aswad *falaj* and the obtained discharge with the subsurface dam, respectively. The historical and augmented time-series of the Al-Aswad *falaj* discharge were classified as dry, normal, and wet categories using a 12-month Standardized Streamflow Index (SSI). Then, an IS risk-based optimization model using the concept of CVaR was formulated to achieve the optimal IS for the three categories under the historical and augmented discharge of the Al-Aswad *falaj*.

$$\text{minimize}: CVaR_{\alpha}^{sh} = VaR_{\alpha} + \frac{1}{1-\alpha}\frac{1}{12Y}\sum_{y=1}^{Y}\sum_{m=1}^{12}\sum_{z=1}^{3}(RD_{y,m,z} - VaR_{\alpha}) \quad (1)$$

Subject to:

$$RD_{y,m,z} = \frac{\max\left\{0, AW_{y,m,z} - DW_{y,m,z}\right\}}{DW_{y,m,z}} \quad (2)$$

$$AW_{y,m,z} = EA \times EC \times DS_{y,m} \times HR_{z} \times DM_{z} \quad (3)$$

$$DM_{z} = \frac{30}{DD_{z}} \quad (4)$$

where:

α=95%

$RD_{y,m,z}$ is the ratio of shortage in zone z in m^{th} month of y^{th} year (-).

$AW_{y,m,z}$ is the allocated water to zone z in m^{th} month of y^{th} year (m^3).

$DW_{y,m,z}$ is the water demand of zone z in m^{th} month of y^{th} year (m^3).

EA and EC are irrigation application and conveyance efficiencies, respectively (%).

$DS_{y,m}$ is the discharge of Al-Aswad *falaj* in m^{th} month of year y (m^3/hr).

HR_z is the irrigation duration for zone z (hr).

DM_z is the irrigation frequency or the number of times in a month that zone z receives water from Al-Aswad *falaj* (-).

DD_z is the interval between two successive irrigation in zone z (day).

Eq. 1 is the objective function of the optimization model, and the constraints are defined in Eqs. 2-4. The decision variables of this model include the irrigation duration and interval of the three zones (i.e. HR_z and DD_z). Through this model, we can obtain the optimal IS during the dry, normal, and wet years, while we can compare the average amount of water shortage in the worst 5% of cases given the historical and augmented discharge of the Al-Aswad *falaj*.

3. RESULTS AND DISCUSSION

3.1. THE CALIBRATION OF THE GROUNDWATER FLOW MODEL

The calibration of the groundwater model was first performed for the steady-state condition, whereby hydraulic conductivity was adjusted to achieve the spatial distribution of calibrated groundwater levels and hydraulic conductivity values. The measured R^2 of 0.98 and RMSE of 0.42 m, between the observed and the simulated groundwater levels, suggest that the accuracy of the steady-state calibrated model is acceptable for the study area with drastic hydrogeological diversity. Table S3 (SI section 4) presents the calibrated hydraulic conductivity values for the available geological units in the study area. The alluvium unit was further divided into three sub-units, namely, alluvial terrace, alluvial fan, and recent wadi

alluvium in the steady-state calibrated model. The recent wadi alluvium unit is composed of coarse to medium Quaternary deposits, which is located within active wadi channels crossing the region; therefore, it has the highest hydraulic conductivity. As shown in Table S3, the hydraulic conductivity values of the wadi alluvium, alluvium fan, and alluvia terrace are 86, 34, and 25.4 m day^{-1}, while Tertiary, ophiolite, HSG, and Huqf units have a conductivity of 2.74, 0.43, 4.74, and 0.15 m day^{-1}, respectively. Moreover, the Al-Aswad *falaj* discharge was simulated using a drain package in which the observed and simulated discharge are respectively 4,620 (53.5) and 4,682 (54.2) m^3 day^{-1} (L S^{-1}).

From the steady-state calibrated model, hydraulic conductivity was obtained for the transient model, which was conducted from Feb. 1991 to Dec. 2016. The calibrated specific yield and specific storage from the transient model are given in Table S3. It can be seen that the specific yield decreased from 0.15 of the wadi alluvium to 0.10 and 0.05 of the alluvial fan and alluvial terrace units, respectively. A value of 0.001 was estimated for the other eight units. A uniform value of 2.9×10^{-5} and 1.9×10^{-4} m^{-1} was estimated for specific storage for the alluvium and hardrock geologic units, respectively. The statistic indicators measuring the accuracy of the calibrated transient model are presented in Table 1. Considering the extreme geographic variations between the mountains and coastal plains and the geologic complexity characterized by Pre-Permian and Quaternary age rocks, an RMSE of 0.74 m and R^2 of 0.86 for groundwater levels and 7.5 LS^{-1} and 0.87 for discharge of the Al-Aswad *falaj* suggest reasonable accuracy.

Table 1. The model statistic indicators for the groundwater model calibration and validation

Period	Groundwater level		Discharge of Al-Aswad *falaj*	
	Weighted RMSE (m)	Weighted R^2	RMSE (LS^{-1})	R^2
Calibration	0.74	0.86	7.5	0.87
Validation	0.82	0.76	8.7	0.74

The simulated and observed groundwater level contour lines were plotted for the last time step of the calibration period (Dec. 2014). As shown in Fig. S3 (SI section 4), the patterns of the simulated and observed groundwater levels are similar, suggesting high accuracy of the calibrated model for such a large area (1,264 km^2) with severe hydrogeological heterogeneity, anisotropy, and high fracture-matrix structural complexity. Fig. 4 compares the time series of *falaj* discharge and groundwater levels between the observed and simulated values. As shown in Fig. 4, three observation wells represent the values from the mountainous, piedmont, and coastal zones, respectively, and hence can be used to monitor accurately the subsurface water movement from the mountainous to coastal zones (Fig. 1). Although groundwater level data have only been recorded since 2012, Al-Aswad *falaj* discharge data were observed from 1991 and, thus, were considered in the calibration period. The well-matched groundwater levels and *falaj* discharge between the simulation and observations indicate that the transient calibrated model can capture the hydraulic dynamics in this complex hardrock-alluvium flow system.

Groundwater levels and discharge of the Al-Aswad *falaj* according to the validated model are as good as those from the calibration model, as shown in Table 1 and Fig. 4, indicating the model's predictive ability. Further, the RMSE values for groundwater levels and *falaj* discharge are respectively 0.82 m and 8.7 LS^{-1}, which are reasonable considering the complex structure of hardrock-alluvium throughout the study area and the model resolution. According to Table S4 (SI section 5), the long-term recharge of 28.1 $Mm^3\ yr^{-1}$ is primarily due to natural rainfall, runoff, and leakage from municipal water networks.

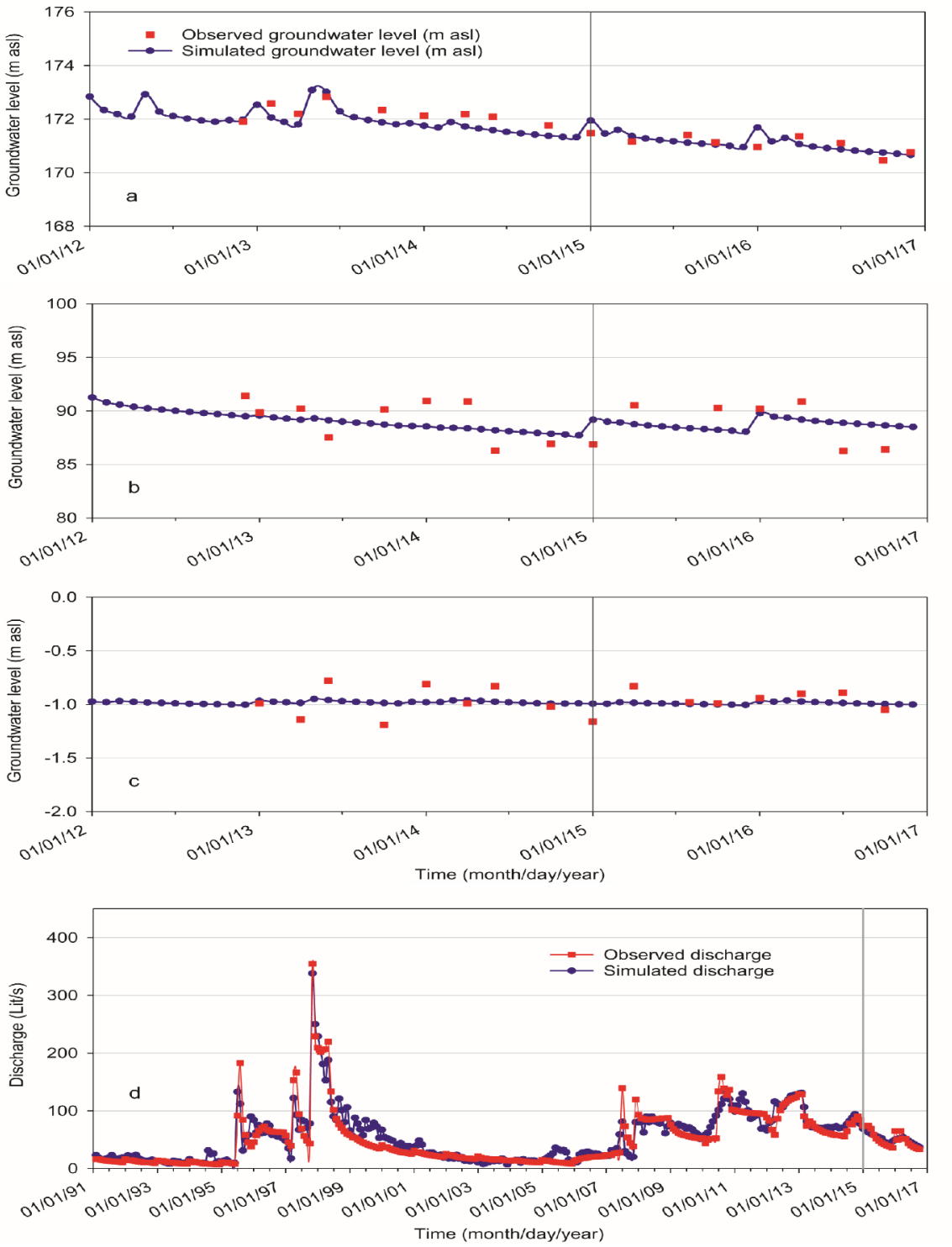

Fig. 4. *Time series of observed and simulated groundwater levels and discharge of Al-Aswad falaj during the calibration (February 1991 to December 2014), and validation (January 2015 to December 2016) periods for: (a) D-3D; (b) WA-15(43); and (c) QT-1 observation wells and (d) Al-Aswad falaj.*

3.2. THE EFFECT OF SUBSURFACE DAM ON DISCHARGE OF AL-ASWAD FALAJ

The validated groundwater model was employed to assess the effects of a subsurface dam on the discharge of the Al-Aswad *falaj*. As stated earlier, the HFB package was applied, in which the optimal hydraulic conductivity and thickness of the subsurface dam are respectively estimated to be 10^{-9} m s^{-1} and 0.5 m in order to achieve a maximum increase in discharge of the Al-Aswad *falaj*. Fig. 3b presents the simulated discharge of the Al-Aswad *falaj* with the construction of the subsurface dam (augmented discharge), in which the long-term average discharge is increased by 46.51%. This augmented discharge can be used to optimize irrigation scheduling to minimize the water shortage in different climates.

3.3. OPTIMAL IRRIGATION SCHEDULING FOR THE AUGMENTED DISCHARGE OF AL-ASWAD FALAJ

As stated earlier, the historical and augmented time series of the Al-Aswad *falaj* discharge are divided into three categories (dry, normal, and wet) based on their 12-month SSI. The years with SSI<-0.5 are considered dry periods, while those with -0.5<SSI<0.5 and SSI>0.5 are considered normal and wet periods, respectively. Table S5 (SI section 6) shows the average daily discharge and the values of 12-month SSI for the historical and augmented discharge, respectively, in which both historical and augmented discharge time series have 7 dry, 10 normal, and 7 wet years. The risk-based optimization model was then applied to each category of the augmented discharge time-series to obtain the optimal IS including the optimal irrigation interval and duration for each zone. This single-objective optimization model was solved using the Genetic Algorithm (GA) (Holland, 1992). The obtained IS with the respective $CVaR_{0.95}^{sh}$, and the current IS of the area with the associated $CVaR_{0.95}^{sh}$ are provided in Table 2.

Table 2. The obtained values of irrigation interval and irrigation duration for each zone, and the weighted average of water shortage in the worst 5% of cases during the dry, normal, and wet years of the historical and augmented discharge of Al-Aswad *falaj*.

Discharge	Climatic condition	Irrigation interval (day)	Irrigation duration (hour)			$CVaR_{0.95}^{sh}$
			Zone 1	Zone 2	Zone 3	
Historical discharge	Dry	6	24	24	96	0.87
	Normal	6	24	24	96	0.75
	Wet	6	24	24	96	0.32
Augmented discharge	Dry	4	25	19	51	0.53
	Normal	5	29	28	63	0.32
	Wet	4	21	18	57	0

As shown in Table 2, the currently practiced irrigation interval is 6 days, regardless of the climatic condition. The obtained optimal irrigation interval and duration under augmented discharge are significantly smaller than the historical discharge. The irrigation intervals for the augmented discharge are respectively 4, 5, and 4 days for dry, normal and wet periods compared to the historical discharge, which is 6 days for all climatic conditions. The notable achievement of the risk-based optimization model is demonstrated in the last column of Table 2. Specifically, it was found that the percentage of water shortage in 5% of the worst cases decreased from 87%, 75%, and 32% under the historical discharge to 53%, 32%, and 0% under the augmented discharge in dry, normal, and wet periods, respectively. In fact, the risk-based optimization model decreased the risk of water shortage by 39.1%, 57.3%, and 100% during the dry, normal, and wet periods using the augmented discharge, which is obtained through the subsurface dam. Moreover, the monthly time-series of water shortage for historical discharge with the currently practiced IS (HS) and augmented discharge with the optimal IS (AS) for dry, normal, and wet years are presented in Fig. 8. It can also be seen that the "average monthly water shortage" of respectively 75%, 26%, and 5% for historical discharge using the currently practiced IS for dry, normal, and wet years

is considerably decreased to 31%, 7%, and 0% for the augmented discharge with the optimal IS. An important point to mention here is that the ratio of water shortage is very high in wet years under the historical discharge and currently practiced IS (Fig. S4 in section 6). This clearly indicates that the applied IS is not optimal, and a significant amount of water is overused because of the low efficiency of the implemented basin surface irrigation system in the study area.

4. CONCLUSION

This study proposes a risk-based simulation-optimization framework to investigate and understand the effects of subsurface dams on groundwater flow and, particularly, the discharge of the Al-Aswad *falaj* through detailed groundwater flow modeling. Then, an optimal IS was obtained from the proposed model to minimize the risk of water shortage for the augmented discharge of the Al-Aswad *falaj*, which is used for the irrigation of downstream agricultural zones. The proposed framework shows a significant increase of 46.51% in the discharge of the Al-Aswad *falaj* and decreased risk of water shortage by 39.1%, 57.3%, and 100% during the dry, normal, and wet periods.

Although the water shortage is markedly decreased in all climatic conditions, shortage during the severe dry years remains a concern. To completely relieve the effects of drought on the downstream agricultural zones, further efforts are needed. The currently practiced irrigation system in the study area is traditional basin surface irrigation with very low conveyance and applied irrigation efficiency. Therefore, the effects of the transition from the current irrigation system to an advanced irrigation system using the agent-based modeling approach should be examined in future studies. Because this study is one of the first of its kind to apply a risk-based simulation-optimization framework in water resource allocation under subsurface dams, our findings can provide a basis for other researchers to improve the management of water resource allocation in arid zones with stressed and limited water resources.

Acknowledgements

We acknowledge the Ministry of Agriculture, Fisheries and Water Resources for providing the required data. We also acknowledge local expert Mr. Eng. Ahmed Salim Al-Wahibi for his generous support for *falaj* survey, soil sampling and data collection. Authors extend appreciation to the research Group DR/RG/17.

Funding

The authors would like to thank Sultan Qaboos University for the financial support under grant number IG/DVC/WRC/18/01.

Authors' Contributions

A.I.: Project administration, Supervision, Funding acquisition, Conceptualization, Methodology, Investigation, Writing-original draft; **M.S.K.:** Software, Investigation, Formal analysis, Writing-original draft; **M.R.N.:** Conceptualization, Methodology, Software, Investigation, Formal analysis, Writing - Review & Editing; **A.A.:** Resources, Writing - Review & Editing; **M.C.:** Formal analysis, Writing - Review & Editing; **H.A.:** Investigation; **A.H.G.:** Writing - Review & Editing.

Availability of Data and Material

The data that support the findings of this study are available from the corresponding author upon reasonable request.

Declarations

Ethics Approval Not applicable.

Consent to Participate Not applicable.

Consent to Publish Not applicable.

Conflicts of Interest/Competing Interests The authors declare that there is no conflict of interest.

References

Adham AKM, Kobayashi A, Murakami A (2011) Effect of climatic change on groundwater quality around the subsurface dam. International Journal of GEOMATE 1:25-32.

Ahmadi T, Ziaei AN, Davary K, Faridhosseini A, Izady A (2012) Estimation of groundwater recharge using various methods in Neishaboor Plain, Iran. IAHR International Groundwater Symposium, November 2012, Kuwait

Ahmadi T, Ziaei AN, Rasoulzadeh A, Davary K, Esmaili K, Izady A (2015) Mapping groundwater recharge areas using CRD and RIB methods in the semi-arid Neishaboor Plain, Iran. Arabian Journal of Geosciences 8(5):2921-2935

Al Marshudi A (2007) Institutional arrangement and water rights in Aflaj systems in the Sultanate of Oman. Proceedings of the International History Seminar on Irrigation and Drainage. Teheran, Iran. P31-42.

Allen RG, Pereira LS, Raes D, Smith M (1998) Crop evapotranspiration-Guidelines for computing crop water requirements-FAO Irrigation and drainage paper 56. FAO, Rome, 300(9):D05109.

Al-Nahari AA (2004) Using subsurface dams for wastewater treatment and reuse. Baylor University.

Armanuos AM, Ibrahim MG, Mahmod WE, Takemura J, Yoshimura C (2019) Analysing the combined effect of barrier wall and freshwater injection countermeasures on controlling saltwater intrusion in unconfined coastal aquifer systems. Water Resources Management 33(4):1265-1280.

Bondoc MD (1986) An overview of alternative remediation methods for groundwater contamination. BSc project, The Ohio State University.

Doherty J (1998) PEST: Model Independent Parameter Estimation, User's Manual; Watermark Computing: Brisbane, Australia.

dos Santos Gomes JL, Vieira FP, Hamza VM (2018) Use of electrical resistivity tomography in selection of sites for underground dams in a semiarid region in southeastern Brazil. Groundwater for Sustainable Development 7:232-238. https://doi.org/10.1016/j.gsd.2018.06.001

Du Preez D (2018) Feasibility and geotechnical design of subsurface dams in dry ephemeral rivers for the augmentation of shallow groundwater supply. Doctoral dissertation, Stellenbosch University.

El-Hames AS (2012) Determination of the transient water table rise behind constructed underground dams. Arabian Journal of Geosciences 5(6):1359-1366. https://doi.org/10.1007/s12517-011-0299-2

Forzieri G, Gardenti M, Caparrini F, Castelli F (2008) A methodology for the pre-selection of suitable sites for surface and underground small dams in arid areas: A case study in the region of Kidal, Mali. Physics and Chemistry of the Earth, Parts A/B/C 33(1-2):74-85. https://doi.org/10.1016/j.pce.2007.04.014

Gibb A (1976) Water resources survey of Northern Oman. Final Report, Directorate General of Finance, Sultanate of Oman.

Glennie KW, Boeuf MGA, Clarke MWH, Moody-Stuart M, Pilaar WFH, Reinhardt BM (1974) Geology of the Oman Mountains. Ministry of Regional Municipalities and Water Resources, Sultanate of Oman.

Holland JH (1992) Genetic algorithms. Scientific American 267(1):66-73

Hut R, Ertsen M, Joeman N, Vergeer N, Winsemius H, van de Giesen N (2008) Effects of sand storage dams on groundwater levels with examples from Kenya. Physics and Chemistry of the Earth, Parts A/B/C 33(1-2):56-66. https://doi.org/10.1016/j.pce.2007.04.006

Ishida S, Tsuchihara T, Imaizumi M (2006) Fluctuation of NO3-N in groundwater of the reservoir of the Sunagawa subsurface dam, Miyako Island, Japan. Paddy and Water Environment 4(2):101-110. https://doi.org/10.1007/s10333-006-0037-7

Izady A, Abdalla O, Joodavi A, Karimi A, Chen M, Tompson A (2017) Groundwater recharge estimation in arid hardrock- alluvium aquifers using combined water- table fluctuation and groundwater balance approaches. Hydrological Processes 31(19):3437-3451. https://doi.org/10.1002/hyp.11270

Izady A, Davary K, Alizadeh A, Ziaei AN, Alipoor A, Joodavi A, Brusseau ML (2014) A framework toward developing a groundwater conceptual model. Arabian Journal of Geosciences 7(9):3611-3631. https://doi.org/10.1007/s12517-013-0971-9

Izady A, Nikoo MR, Bakhtiari PH, Baawain MS, Al-Mamari H, Msagati TA, Nkambule TT, Al-Maktoumi A, Chen M, Prigent S (2020) Risk-based stochastic optimization of evaporation ponds as a cost-effective and environmentally-friendly solution for the disposal of oil-produced water. Journal of Water Process Engineering, 38:101607. https://doi.org/10.1016/j.jwpe.2020.101607

Jamali IA, Mörtberg U, Olofsson B, Shafique M (2014) A spatial multi-criteria analysis approach for locating suitable sites for construction of subsurface dams in Northern Pakistan. Water Resources Management 28(14):5157-5174.

Kabiri-Samani A, Shams MR (2014) Discharge coefficient of subsurface weirs. Proceedings of the Institution of Civil Engineers-Water Management 167(4):187-193. https://doi.org/10.1680/wama.12.00050

Kim JT, Choo CO, Kim MI, Jeong GC (2017) Validity evaluation of a groundwater dam in Oshipcheon River, eastern Korea using a SWAT–MODFLOW model. Environmental Earth Sciences 76(22):769. https://doi.org/10.1007/s12665-017-7085-8

Knorr G, Stollberg R, Raju NJ, Wycisk P, Gossel W (2016) Prevention of groundwater wells from salinization by subsurface dams. Hallesches Jahrbuch für Geowissenschaften 38:55-66.

Lalehzari R, Tabatabaei SH (2015) Simulating the impact of subsurface dam construction on the change of nitrate distribution. Environmental Earth Sciences 74(4):3241-3249. https://doi.org/10.1007/s12665-015-4362-2

Li M, Zheng T, Zhang J, Fang Y, Liu J, Zheng X, Peng H (2019) A new risk assessment system based on set pair analysis–variable fuzzy sets for underground reservoirs. Water Resources Management 33(15):4997-5014.

Macdonald M (1985) Wadi Aday wellfield improvement works contract. Final report, volume 3 appendices B, C, D & E. Ministry of Electricity and Water, Sultanate of Oman.

Nawa N, Miyazaki K (2009) The analysis of saltwater intrusion through Komesu underground dam and water quality management for salinity. Paddy and Water Environment 7(2):71-82. https://doi.org/10.1007/s10333-009-0154-1

Nazarieh F, Ansari H, Ziaei AN, Izady A, Davari K, Brunner P (2018) Spatial and temporal dynamics of deep percolation, lag time and recharge in an irrigated semi-arid region. Hydrogeology Journal 26(7):2507-2520

Nishigaki M, Kankam-Yeboah K, Komatsu M (2004) Underground dam technology in some parts of the world. Journal of Groundwater Hydrology 46(2):113-130. https://doi.org/10.5917/jagh1987.46.113

Panday S, Langevin CD, Niswonger RG, Ibaraki, M, Hughes JD (2013) MODFLOW–USG version 1: An unstructured grid version of MODFLOW for simulating groundwater flow and tightly coupled processes using a control volume finite-difference formulation: U.S. Geological Survey Techniques and Methods, book 6, chap. A45, 66 p.

Rockafellar RT, Uryasev S (2000) Optimization of conditional value-at-risk. Journal of Risk 2(3):21-41. DOI: 10.21314/JOR.2000.038

Rohina A, Ahmadi H, Moeini A, Shahriv A (2020) Site selection for constructing groundwater dams through Boolean logic and AHP method (case study: watershed of Imamzadeh Jafar Gachsaran). Paddy and Water Environment 18(1):59-72. https://doi.org/10.1007/s10333-019-00764-9

Senthilkumar M, Elango L (2011) Modelling the impact of a subsurface barrier on groundwater flow in the lower Palar River basin, southern India. Hydrogeology Journal 19(4):917. https://doi.org/10.1007/s10040-011-0735-0

Smith RO (1984) Results of exploration drilling and water well completion in the wadi Aday, Greater Capital Area. Public Authority for Water Resources, Sultanate of Oman.

Zarkesh MMK, Ata, D, Jamshidi A (2012) Performance of underground dams as a solution for sustainable management of drought. JBU 1:35-45.

Supplementary Information (SI)

SI. S1. Aflaj: An Ancient Water Supply System

A *falaj* (also known as *qanat* (Iran), *qanat romani* (Jordan and Syria), *karez* (Afghanistan and Pakistan), *kanerjing* (China), *khettara* (Morocco), *foggara* (North Africa), *galerias* (Spain)) is an ancient water supply system in which a long horizontal tunnel with a length of several kilometers is dug several meters underground (Al Amri et al., 2014). *Falaj* (plural *aflaj*) comes from an Arabic word that means 'split into parts' since it divides water between farms. A *falaj* does not use machines to extract water, but instead, obtains water from underground sources and depends on gravity to force water to flow through its channels. While water is constantly streaming in *aflaj* year long, the fullness of a *falaj* depends on the rainy seasons and, thus, determines the fullness of the water sources.

A *falaj* consists of four main parts: the *mother well*, access shafts, tunnel, and *outlet*. The main source of water is located in the *mother well*, in which the water has the highest quality. Then, the water flows from the mother *well* to the *outlet* through the tunnel. The length of the tunnel depends on the type of terrain where the *falaj* runs, the amount of water in the *mother well*, and distance to the final water destination. The access shafts are built every 20 meters along the tunnel to facilitate

ventilation and to help in the removal of debris. A ring of burnt clay is constructed at the shaft mouth in order to prevent the destruction of the *falaj* if the tunnel collapses and flooding water from entering the *falaj*. These covered rings also protect water from pollutants and avert people and animals from falling into the *falaj*.

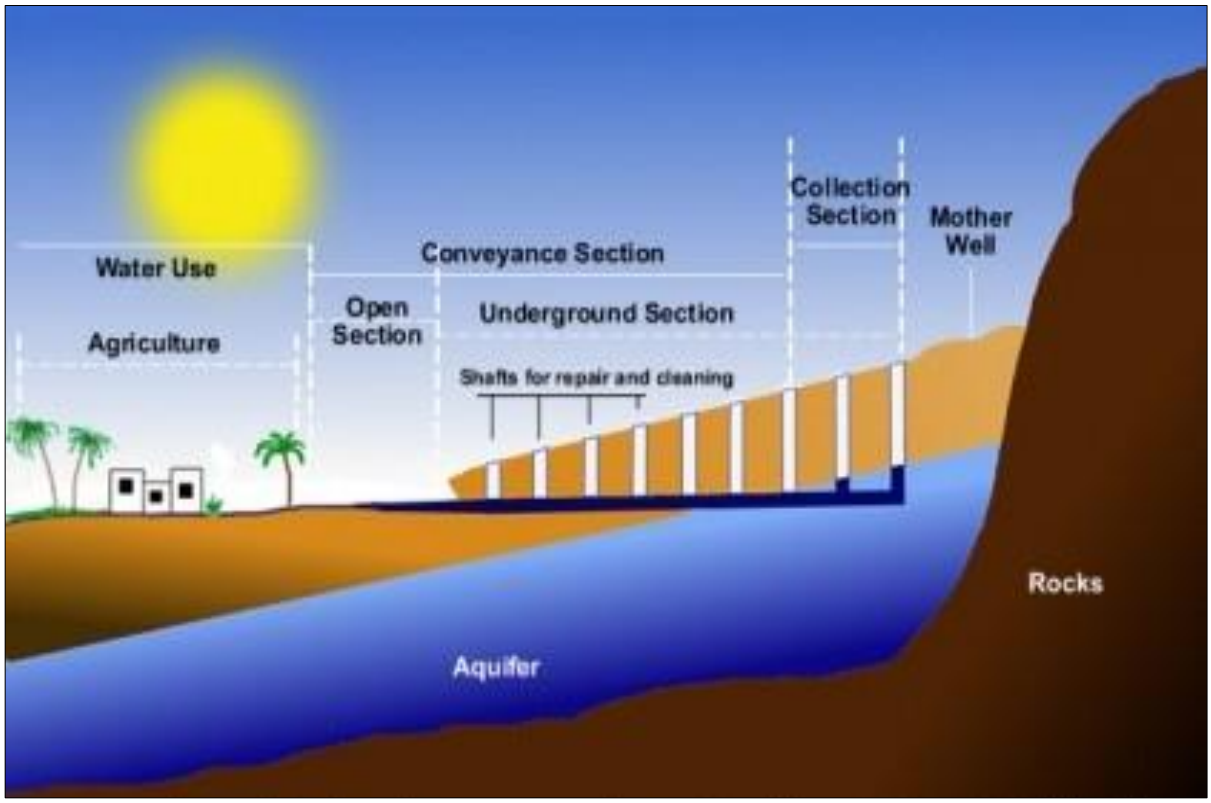

Fig. S1. *Longitudinal cross section of a falaj (Adapted from https://www.azimuthproject.org/azimuth/show/Qanat)*

SI. S2. Groundwater Conceptual Model

The framework proposed by Izady et al. (2014) was used for developing the groundwater conceptual model of the study area. The groundwater flow originates from the southwest of the study area and reaches to the northeast of the study area at sea level. The data of 90 boreholes were used to generate a three-dimensional stratigraphic model of the five principal hydrogeological units, including

Huqf, HSG, Ophiolite, Tertiary, and alluvium geologic units (Fig. S2). The thickness of the stratigraphic model ranges from 240 to 600 m throughout the study area, where the alluvium thickness varies between 20 and 74 m (Smith 1984; Macdonald 1985). A constant head of zero is considered for the coastline boundary along the coast of the Oman Sea in the northeast of the study area. The highlands of the NOMs, which are situated at the southwest boundary of the study area, represent a groundwater and surface water divide. No-flux boundary condition is presumed for the east and west boundaries since they are parallel to the direction of the groundwater flow. According to the aquifer test results, the alluvium hydraulic conductivity varies between 20 to 100 m day^{-1} and specific yield ranges 0.05-0.15. The Tertiary geologic unit has a specific yield of 0.005 and hydraulic conductivity of 2.74 m day^{-1}, while those of the Ophiolite formation are 0.001 and 0.43 m day^{-1}. The HSG has the highest hydrodynamic properties compared with other hardrock formations, with a specific yield of 0.008 and hydraulic conductivity of 4.74 m day^{-1}. For the Huqf group, specific yield and hydraulic conductivity are estimated to be 0.15 m day^{-1} and 0.001, respectively. The annual groundwater abstraction for irrigation and domestic consumptions is estimated to be 14.6 Mm^3 from the wells and 5.1 Mm^3 from the wellfield. The water-table fluctuation-based approach, proposed by Izady et al. (2017), was employed to estimate the recharge rates resulting from rainfall, runoff, evapotranspiration, abstraction, and leakage from the public water distribution network. The estimated values were used as initial values for groundwater recharge in the modeling. All required data for the groundwater modeling is obtained from the Ministry of Agriculture, Fisheries, and Water Resources, Oman.

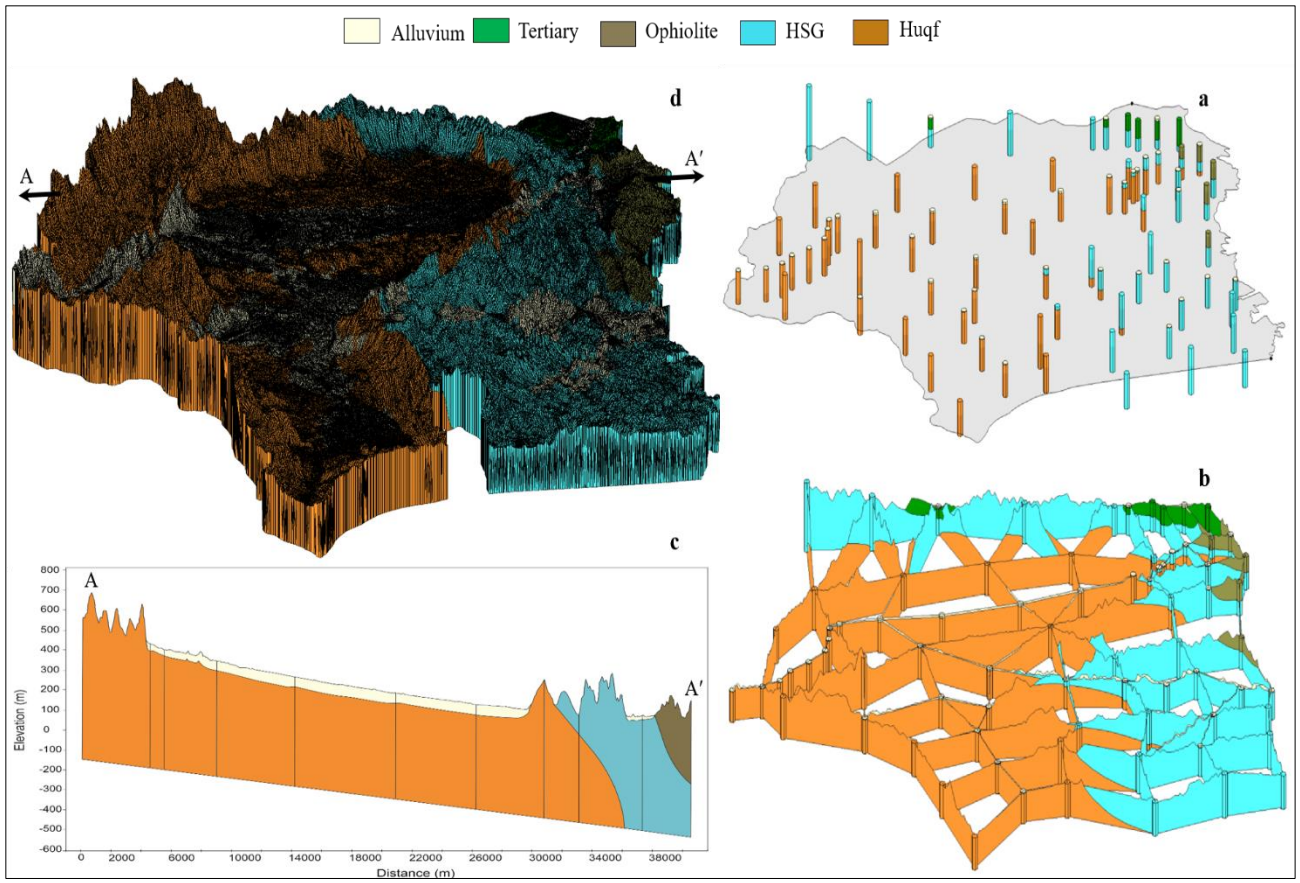

Fig. S2. *Stratigraphic model: (a) and (b) Boreholes and cross sections used to construct stratigraphy of the groundwater modeling domain; (c) Horizontal cross-section A-A'; (d) A three-dimensional (3D) stratigraphic model for the groundwater modeling domain*

SI. S3. Crops Water Requirement

To calculate the crops water requirement (CWR), we utilized the FAO Penman-Monteith method (Allen et al. 1998). In the first step, reference evapotranspiration (ET_0) is calculated using Eq. S1 based on the local meteorological data. Eq. S1 includes different terms that should be calculated for each month to obtain dynamic monthly ET_0. The calculated terms along with ET_0 are provided in Table S1 for year 1992, as an example.

$$ET_0 = \frac{0.408\Delta\left(R_n - G\right) + \gamma \frac{900}{T+273} u_2 \left(e_s - e_a\right)}{\Delta + \gamma\left(1 + 0.34u_2\right)} \quad \text{(S1)}$$

where:

ET_0: Reference evapotranspiration [mm day^{-1}]

R_n: Net radiation at the crop surface [MJ m^{-2} day^{-1}]

G: Soil heat flux density [MJ m^{-2} day^{-1}]

T: Mean daily air temperature at 2 m height [$^{\circ}$C]

u_2: Wind speed at 2 m height [m s^{-1}]

e_s: Saturation vapor pressure [kPa]

e_a: Actual vapor pressure [kPa]

Δ: Slope of saturation vapor pressure curve [kPa $^{\circ}$C^{-1}]

γ: Psychrometric constant [kPa $^{\circ}$C^{-1}]

Table S1. *Monthly values of terms needed for the calculation of reference evapotranspiration (ET_0) for year 1992, as an example.*

Year	Month	R_n $(\frac{MJ}{m^2 day})$	G $(\frac{MJ}{m^2 day})$	T (℃)	u_2 $(\frac{m}{s})$	e_s (kPa)	e_a (kPa)	Δ $(\frac{kPa}{℃})$	γ $(\frac{kPa}{℃})$	ET_0 $(\frac{mm}{day})$
	January	11.41	0	13.58	1.43	2.25	1.35	0.17	0.06	2.37
	February	17.94	0.25	22.98	2	3.01	1.5	0.18	0.07	4.2
	March	20.06	0.49	26.48	1.99	3.68	1.55	0.21	0.07	5.41
	April	22.75	0.7	31.47	2.07	4.83	1.42	0.27	0.07	6.96
	May	23.87	0.7	36.59	2.2	6.18	1.47	0.35	0.07	8.1
1992	June	23.87	0.21	38.06	2.21	6.71	1.92	0.37	0.07	8.41
	July	22.55	0	37.54	2.32	6.49	2.42	0.36	0.07	8.07
	August	22.43	0	35.99	2.34	6.17	2.39	0.33	0.07	7.83
	September	21.34	0	34.52	1.93	5.64	2.23	0.31	0.07	6.79
	October	19.44	0	31.02	1.66	4.67	1.85	0.27	0.07	5.51
	November	14.84	0	26.6	1.52	3.23	2.06	0.21	0.07	3.35
	December	14.81	0	22	1.48	2.77	1.56	0.17	0.07	3.26

The next step is to calculate the crops evapotranspiration (ET_C) using Eq. S2:

$$ET_c = K_c \times ET_0 \quad \text{(S2)}$$

where,

K_c is crop coefficient which is respectively considered 0.96, 0.64, 1.1, and 1.2 for date palm trees, lemon, banana, and corn silage, according to Allen et al. (1998). Through the calculation of CWR, the amount of net water demand for the three zones is determined. Then, the gross water demand of each zone is calculated using the irrigation perimeter and water conveyance and application efficiencies, which are 80% and 60%, respectively. It should be mentioned that the irrigation perimeter for each date palm and lemon tree is 23 and 12.56 m^2, respectively. Banana is cultivated in 5% of the area in zone 3, while the number of lemon trees in the same area is 25. The number of date palm trees in zones 1, 2, and 3 are 1,096, 1,117, and 3,410, respectively, while 100%, 90%, and 85% of the area of zones 1, 2, and 3 are intercropped with date palm and corn silage. Using this information, the calculated water demands of the three zones for 1992 are presented in Table S2, as an example.

Table S2. *Net and gross water demands of the three zones for year 1992, as an example.*

Year	Month	Net Water Demand				Gross Water Demand			
		Zone 1 ($L\ S^{-1}$)	Zone 2 ($L\ S^{-1}$)	Zone 3 ($L\ S^{-1}$)	Total ($L\ S^{-1}$)	Zone 1 ($L\ S^{-1}$)	Zone 2 ($L\ S^{-1}$)	Zone 3 ($L\ S^{-1}$)	Total ($L\ S^{-1}$)
1992	January	2.31	1.77	6.57	10.65	4.82	3.69	13.68	22.19
	February	4.16	3.18	11.79	19.13	8.66	6.62	24.57	39.85
	March	5.19	3.97	14.72	23.88	10.81	8.26	30.66	49.73
	April	6.7	5.12	18.99	30.81	13.95	10.66	39.57	64.18
	May	7.81	5.97	22.15	35.93	16.26	12.43	46.13	74.82
	June	8.11	6.2	23	37.31	16.89	12.91	47.91	77.71
	July	7.78	5.95	22.08	35.81	16.22	12.4	46.01	74.63
	August	7.55	5.77	21.41	34.73	15.72	12.02	44.6	72.34
	September	6.52	4.99	18.51	30.02	13.59	10.39	38.56	62.54
	October	5.29	4.04	14.99	24.32	11.01	8.42	31.24	50.67
	November	3.2	2.45	9.08	14.73	6.67	5.1	18.91	30.68
	December	2.98	2.28	8.46	13.72	6.21	4.75	17.63	28.59

SI. S4. The Calibration of Groundwater Flow Model

Table S3 presents the calibrated hydraulic conductivity values for the available geological units in the study area.

Table S3. *Calibrated hydrodynamic properties for different geological units.*

Geological unit	Hydraulic conductivity ($m\ day^{-1}$)	Specific yield	Specific storage (m^{-1})
Wadi alluvium	86.0	0.15	2.9×10^{-5}
Alluvial fan	34.0	0.10	2.9×10^{-5}
Alluvia terrace	25.0	0.05	2.9×10^{-5}
Tertiary L1, 2, 3	2.7 (3.2×10^{-5})	0.001	1.9×10^{-4}
Tertiary L4, 5	1.3 (1.6×10^{-5})	0.001	1.9×10^{-4}
Ophiolite L1, 2, 3	0.4 (4.9×10^{-6})	0.001	1.9×10^{-4}
Ophiolite L4, 5	0.2 (2.5×10^{-6})	0.001	1.9×10^{-4}
HSG L1, 2, 3	4.7 (5.5×10^{-5})	0.001	1.9×10^{-4}
HSG L4, 5	1.4 (1.6×10^{-5})	0.001	1.9×10^{-4}
Huqf L1, 2, 3	0.2 (1.7×10^{-6})	0.001	1.9×10^{-4}
Huqf L4, 5	0.1 (1.0×10^{-6})	0.001	1.9×10^{-4}

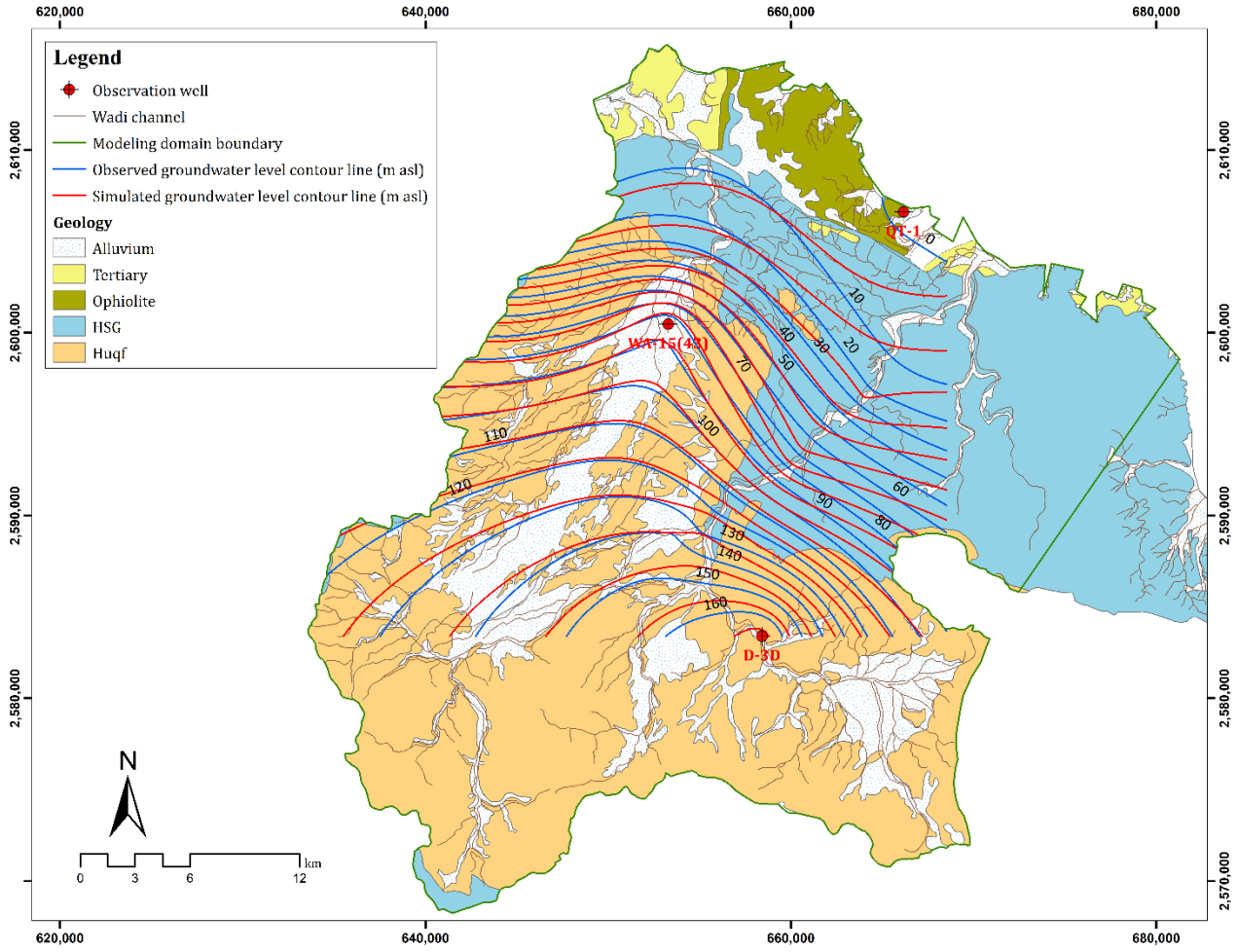

Fig. S3. *The simulated (red line) and observed (blue line) contour lines of groundwater level (December 2014). The starting date of the calibration period is Feb. 1991.*

SI. S5. Transient Groundwater Balance

Table S4 lists the annual groundwater balance components. The long-term recharge of 28.1 Mm^3 yr^{-1} is primarily due to natural rainfall, runoff, and leakage from municipal water networks (Al-Bulushi et. al., 2018). According to Table 3, three peak groundwater recharges in 1997, 2007 and 2010 were caused by heavy rainfalls, while groundwater discharged to the ocean can reach as high as

10.75 Mm^3 yr^{-1}. In addition, the groundwater abstraction from different sources (agriculture and domestic wells, wellfield, and *aflaj*) amounts to 18.39 Mm^3 yr^{-1}.

Table S4. *The components of yearly groundwater balance in million cubic meters*

Period	Inflow		Outflow		Balance
	Recharge	Constant head In	Abstraction	Constant head Out	±ΔV
Jan. 1991 - Dec. 1991	18.37	3.29	16.96	9.28	-4.58
Jan. 1992 - Dec. 1992	18.37	3.29	17.25	9.35	-4.95
Jan. 1993 - Dec. 1993	18.37	3.28	16.26	9.42	-4.03
Jan. 1994 - Dec. 1994	18.37	3.27	16.48	9.51	-4.35
Jan. 1995 - Dec. 1995	36.17	3.28	17.75	9.83	11.86
Jan. 1996 - Dec. 1996	18.41	3.29	18.28	9.42	-5.98
Jan. 1997 - Dec. 1997	65.95	3.27	19.82	10.10	39.30
Jan. 1998 - Dec. 1998	25.74	3.28	20.55	10.08	-1.60
Jan. 1999 - Dec. 1999	9.59	3.24	17.7	9.36	-14.22
Jan. 2000 - Dec. 2000	18.37	3.23	17.28	9.70	-5.39
Jan. 2001 - Dec. 2001	18.37	3.22	17.06	9.85	-5.32
Jan. 2002 - Dec. 2002	18.63	3.21	16.92	9.96	-5.04
Jan. 2003 - Dec. 2003	21.34	3.19	17.72	10.22	-3.41
Jan. 2004 - Dec. 2004	10.47	3.16	17.66	9.56	-13.59
Jan. 2005 - Dec. 2005	19.57	3.14	17.62	9.93	-4.84
Jan. 2006 - Dec. 2006	21.56	3.12	17.85	10.10	-3.28
Jan. 2007 - Dec. 2007	122.1	3.06	18.88	14.52	91.74
Jan. 2008 - Dec. 2008	14.66	3.09	19.97	13.44	-15.67
Jan. 2009 - Dec. 2009	23.56	3.04	19.13	12.48	-5.02
Jan. 2010 - Dec. 2010	73.24	3.00	20.13	13.12	42.98
Jan. 2011 - Dec. 2011	15.85	2.97	20.30	11.94	-13.43
Jan. 2012 - Dec. 2012	31.97	2.89	20.36	12.16	2.32
Jan. 2013 - Dec. 2013	28.60	2.85	19.81	11.73	-0.08
Jan. 2014 - Dec. 2014	17.97	2.85	19.80	11.2	-10.17
Jan. 2015 - Dec. 2015	20.50	2.87	20.08	11.41	-8.13
Jan. 2016 - Dec. 2016	24.52	2.84	16.60	11.78	-1.02
26-year average	**28.1**	**3.12**	**18.39**	**10.75**	**2.07**

SI. S6. Optimal Irrigation Scheduling for the Augmented Discharge of Al-Aswad Falaj

Table S5 shows the average daily discharge and the values of 12-month SSI for the historical and augmented discharge, respectively, in which both historical and augmented discharge time-series have 7 dry, 10 normal, and 7 wet years.

Table S5. *The average daily discharge of the Al-Aswad falaj for historical and augmented discharge during 1992-2015 and their associated 12-month SSI for the dry, normal and wet categories.*

Year	Mean Daily Discharge ($1000\ m^3\ day^{-1}$)		SSI		Category	
	Historical	Augmented	Historical	Augmented	Historical	Augmented
1992	1.45	2.93	-0.88	-0.73	Dry	Dry
1993	0.94	1.93	-1.99	-1.99	Dry	Dry
1994	1.29	2.73	-1.05	-1.05	Dry	Dry
1995	3.84	5.87	-0.05	-0.15	Normal	Normal
1996	5.52	8.17	0.16	0.16	Normal	Normal
1997	9.55	13.0	1.52	1.52	Wet	Wet
1998	12.43	16.22	1.99	1.99	Wet	Wet
1999	5.97	9.89	0.49	0.60	Normal	Wet
2000	3.80	6.67	-0.16	-0.05	Normal	Normal
2001	2.57	4.72	-0.37	-0.37	Normal	Normal
2002	1.46	2.76	-0.74	-0.88	Dry	Dry
2003	1.03	1.96	-1.52	-1.52	Dry	Dry
2004	1.11	2.30	-1.25	-1.25	Dry	Dry
2005	2.02	4.26	-0.49	-0.49	Normal	Normal
2006	1.99	3.91	-0.61	-0.61	Dry	Dry
2007	3.24	5.29	-0.26	-0.26	Normal	Normal
2008	6.48	8.86	0.61	0.26	Wet	Normal
2009	5.87	8.97	0.37	0.37	Normal	Normal
2010	7.91	11.16	0.88	1.04	Wet	Wet
2011	8.14	10.81	1.05	0.88	Wet	Wet
2012	8.56	12.08	1.25	1.25	Wet	Wet
2013	6.84	10.12	0.74	0.74	Wet	Wet
2014	5.79	9.78	0.26	0.48	Normal	Normal
2015	4.64	7.25	0.05	0.05	Normal	Normal

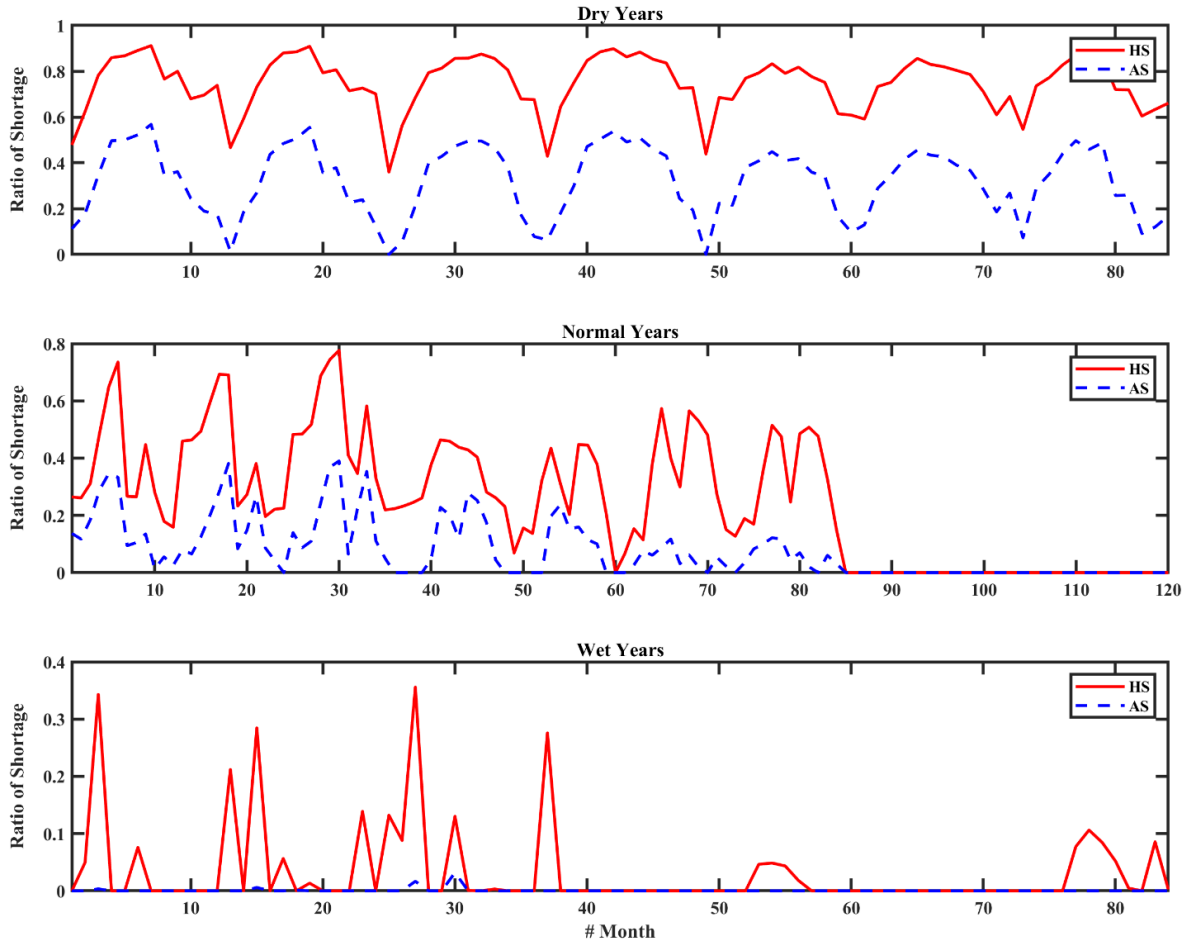

Fig. S4. *The monthly time-series of water shortage for historical discharge with the currently practiced IS (HS) and augmented discharge with the optimal IS (AS) during dry, normal, and wet years*

References

Allen RG, Pereira LS, Raes D, Smith M (1998) Crop Evapotranspiration-Guidelines for computing crop water requirements-FAO. Irrigation and drainage paper 56. FAO, Rome, 300(9):D05109.

Izady A, Abdalla O, Joodavi A, Karimi A, Chen M, Tompson A (2017) Groundwater recharge estimation in arid hardrock- alluvium aquifers using combined water- table fluctuation and groundwater balance approaches. Hydrological Processes 31(19):3437-3451. https://doi.org/10.1002/hyp.11270

Izady A, Davary K, Alizadeh A, Ziaei AN, Alipoor A, Joodavi A, Brusseau ML (2014) A framework toward developing a groundwater conceptual model. Arabian Journal of Geosciences 7(9):3611-3631. https://doi.org/10.1007/s12517-013-0971-9

Macdonald M (1985) Wadi Aday wellfield improvement works contract. Final report, volume 3 appendices B, C, D & E. Ministry of Electricity and Water, Sultanate of Oman.

Smith RO (1984) Results of exploration drilling and water well completion in the wadi Aday, Greater Capital Area. Public Authority for Water Resources, Sultanate of Oman.